UNCLASSIFIED



ORNL-2067
TID-4500 (11th ed.)
Instrumentation
Progress



# INSTRUMENTATION AND CONTROLS DIVISION

# SEMIANNUAL PROGRESS REPORT

# FOR PERIOD ENDING JANUARY 31, 1956



OAK RIDGE NATIONAL LABORATORY
OPERATED BY
UNION CARBIDE NUCLEAR COMPANY
A Division of Union Carbide and Carbon Corporation
UCC
POST OFFICE BOX P · OAK RIDGE, TENNESSEE

UNCLASSIFIED

ORNL-2067
TID-4500 (11th ed.)
Instrumentation
Progress

4

Contract No. W-7405-eng-26

# INSTRUMENTATION AND CONTROLS DIVISION

# SEMIANNUAL PROGRESS REPORT

## For Period Ending January 31, 1956

C. J. Borkowski, Director

DATE ISSUED

MAY 3 1956

OAK RIDGE NATIONAL LABORATORY
Operated by
UNION CARBIDE NUCLEAR COMPANY
A Division of Union Carbide and Carbon Corporation
Post Office Box P
Oak Ridge, Tennessee

ORNL-2067
TID-4500 (11th ed.)
Instrumentation
Progress

## *INTERNAL DISTRIBUTION*

1. C. E. Center
2. Biology Library
3. Health Physics Library
4-6. Central Research Library
7. Reactor Experimental Engineering Library
8-19. Laboratory Records Department
20. Laboratory Records, ORNL R. C.
21. A. M. Weinberg
22. S. J. Cromer
23. L. B. Emlet (K-25)
24. J. P. Murray (Y-12)
25. J. A. Swartout
26. E. H. Taylor
27. E. J. Murphy
28. E. D. Shipley
29. C. S. Harrill
30. F. C. VonderLage
31. W. H. Jordan
32. S. C. Lind
33. F. L. Culler
34. A. H. Snell
35. A. Hollaender
36. M. T. Kelley
37. K. Z. Morgan
38. T. A. Lincoln
39. A. S. Householder
40. C. E. Winters
41. D. W. Cardwell
42. E. M. King
43. G. E. Boyd
44. W. J. Ladniak
45. P. R. Bell
46. C. J. Borkowski
47. G. S. Hurst
48. R. S. Livingston
49. E. E. Fairstein
50. C. W. Sheppard
51. W. G. Stone
52. D. D. Cowen
53. C. P. Keim
54. C. D. Susano
55. P. M. Reyling
56. G. C. Williams
57. M. J. Skinner
58-59. J. V. Francis
60. R. W. Johnson
61. D. J. Fisher
62. E. G. Struxness
63. J. R. McNally, Jr.
64. J. L. Gabbard
65. R. A. Charpie
66. T. V. Blosser
67. E. L. Olson
68. J. A. Auxier
69. R. K. Abele
70. J. R. Tallackson
71. H. E. Banta
72. E. W. Burdette
73. R. R. Dickison
74. ORNL – Y-12 Technical Library, Document Reference Section

## *EXTERNAL DISTRIBUTION*

75-76. Ohio State University (Professor of Naval Science)
77. R. Hofstadter, Stanford University
78. J. C. Nance, Consolidated-Vultee Aircraft Corporation
79. E. A. Rollor, ANP Project Office, Fort Worth
80. R. N. Keller, University of Colorado
81. Division or Research and Development, AEC, ORO
82-471. Given distribution as shown in TID-4500 under Instrumentation category

DISTRIBUTION PAGE TO BE REMOVED IF REPORT IS GIVEN PUBLIC DISTRIBUTION

UNCLASSIFIED

## CONTENTS

# INSTRUMENTATION AND CONTROLS DIVISION SEMIANNUAL PROGRESS REPORT

## DOUBLE DIFFERENTIATION IN RADIATION DETECTION AMPLIFIERS USING RC NETWORKS – A NONBLOCKING COUNTER AMPLIFIER

E. Fairstein

It has been found that the double-line pulse-shaping technique used in radiation detection amplifiers[1,2] results in a number of desirable characteristics, among which are included:

1. rapid recovery of the amplifier from the effects of an overloading signal,
2. elimination of base-line shift with counting rate,
3. simultaneous minimization of noise in the amplifier output and of pileup in the amplifier section preceding the gain control.

It would be desirable to use RC networks in place of the delay lines, since delay lines are relatively expensive, bulky, subject to extraneous electrical pickup, difficult to prepare, and require critically adjusted terminating networks. Unfortunately, RC networks exhibit a number of shortcomings as well:

1. The curvature of the output pulse peak is such that it requires unnecessarily fast circuits in the pulse-height analyzer that usually follows an amplifier.

2. When optimum clipping times are chosen for both the RC and delay-line networks, it is found that the RC network results in an amplifier recovery time that is three to four times longer than that resulting from the use of delay lines.

3. Under high overload conditions, the situation is many times worse. The exponential pulse decay associated with RC networks results in an exaggerated recovery time and an upset in the area balance between positive and negative pulse halves to the extent that the dependence of base-line shift on counting rate is as poor as for the singly differentiating type of pulse shapers.

The first of the above shortcomings is not too serious. A number of simple circuits can be used to flatten the top of the pulse, thus relaxing the speed requirements in circuits following the amplifier.

The second deficiency is more fundamental and is not subject to any appreciable improvement. The resulting limitations on the maximum permissible counting rate is the price paid for the use of simple RC networks.

The third difficulty is usually so serious that the use of RC networks has not been considered practical in the past. However, a circuit technique has been devised that removes this shortcoming from the list of difficulties.

The first RC differentiator is placed at the input of the amplifier chain to minimize pulse pileup effects. A second RC differentiator, whose time constant is identical to the first, is placed in the amplifier chain as far along as possible without causing serious saturation effects in the section between the two differentiators. (The saturation effects are serious only at high counting rates and high overloads.) In a high-gain amplifier, this point is so near to the input of the amplifier that the output sections saturate, causing the difficulty mentioned earlier. A means of avoiding this is to clip the undershoot produced by the second RC network with a diode clamp, and to place a third RC differentiator, having a time constant equal to or shorter than that of the first two, near the output of the amplifier. The second RC network serves to sharply define the pulse width produced by the first and thus prevents an extended recovery time under overload conditions. The diode clamp, although not perfect, limits the amplitude of the undershoot to a value which will not overload later stages of the amplifier. The third RC network assures this condition and at the same time reinstates an undershoot that prevents base-line shift at high counting rates.

The circuit of a counter amplifier suitable for proportional or scintillation counting by the use of this type of pulse shaping is shown in Fig. 1.

[1]E. Fairstein, *Instrument Research and Development Quar. Prog. Rep. Jan. 20, 1952*, ORNL-1335, p 12.

[2]E. Fairstein, *Instrumentation and Controls Semiann. Prog. Rep. Jan. 31, 1955*, ORNL-1865, p 15.

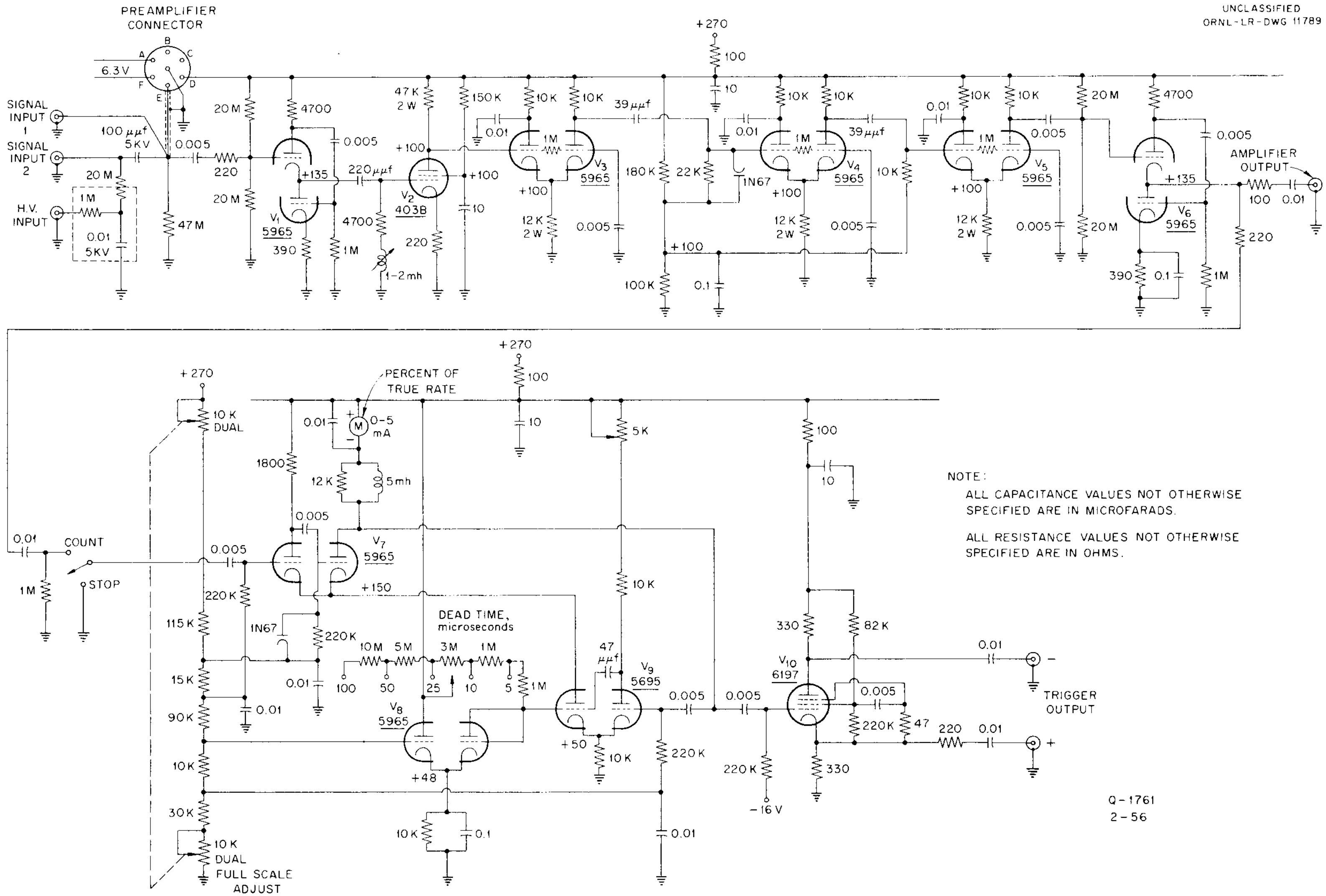


**Fig. 1. Circuit Diagram of Nonblocking Counter Amplifier.**

The amplifier proper uses tubes $V_1$ through $V_6$. The remaining tubes are used in the trigger circuit and power supply.

The input circuit permits direct connection to a proportional counter, to a scintillation counter, or to a preamplifier. Tube $V_1$ is a White cathode follower which provides a low-noise, low-impedance driving circuit for the first differentiator. The differentiator is inductively compensated to reduce the recovery time. The second differentiator is placed between $V_3$ and $V_4$ and is clamped by a germanium diode. The third differentiator is placed between $V_4$ and $V_5$. The first two have a time constant of approximately 1 $\mu$sec, and the last, a time constant of 0.8 $\mu$sec. Tube $V_6$ is a White cathode-follower output stage. Where a general-purpose amplifier is not necessary, the input and output cathode followers can be omitted. The amplifiers, $V_3$ and $V_4$, are cathode-coupled pairs with operating points so chosen that grid current flow does not occur on overload signals. No a-c feedback is used, but the circuit is such that a significant d-c stabilization factor exists, which indirectly stabilizes the a-c gain.

In using the amplifier with a radiation detector, it is necessary that the charge collected at the detector output, which is the result of an ionizing event, leaks off through the external circuit with a time constant of not less than 150 $\mu$sec. A faster leak rate will result in multiple pulsing, unless a trigger dead time of more than 10 $\mu$sec is used.

The performance of the amplifier is shown in Figs. 2 and 3. Figure 2 is a series of oscillograms of the amplifier output taken under conditions of varying amplifier input voltage. The voltage source was a pulse generator. The amplifier trigger sensitivity is fixed at a level corresponding to an input signal threshold of approximately 1.5 mv. The oscillograms show that the amplifier has a usable dynamic range of at least 6000:1, a range that is well in excess of that necessary for the commonly used radiation detectors. The oscillograms also show that the area balance between positive and negative portions of the signal is maintained quite well at all input levels. This condition is reflected in the fixed position of the counting-rate plateau knee at various counting-rate levels. Not so obvious is the rapid recovery from the effects of an overload signal. A test indicated that a 10-mv input signal occurring

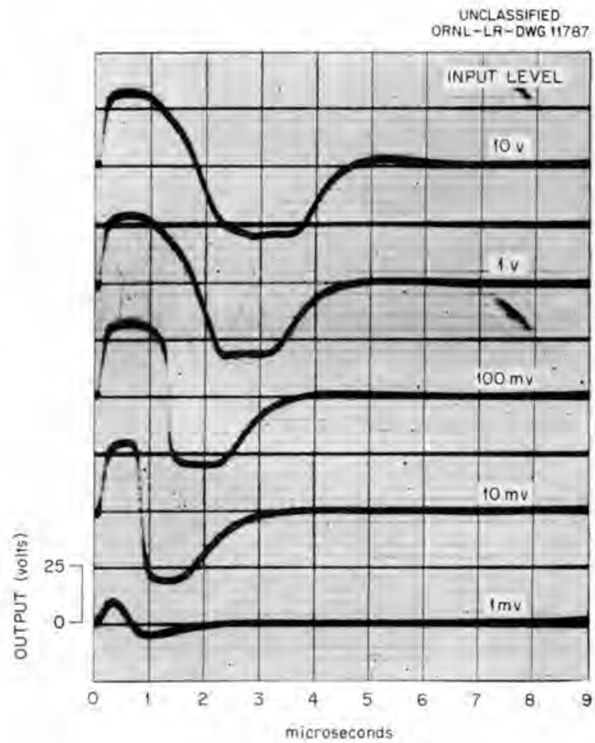


**Fig. 2. Counter-Amplifier Overload Characteristics.**

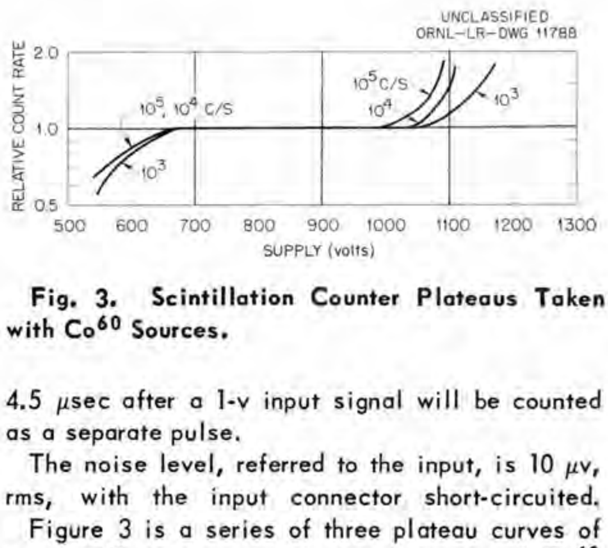


**Fig. 3. Scintillation Counter Plateaus Taken with $Co^{60}$ Sources.**

4.5 $\mu$sec after a 1-v input signal will be counted as a separate pulse.

The noise level, referred to the input, is 10 $\mu$v, rms, with the input connector short-circuited.

Figure 3 is a series of three plateau curves of a scintillation counter facing a series of $Co^{60}$ sources. The curves were normalized for easy comparison and corrected for the 10-$\mu$sec trigger dead time. It should be noted that the correction amounted to 50% for the 100,000-counts/sec curve. The curves show a negligible knee shift and an absence of the dip near the higher voltage end of the plateau which appears with amplifiers that are subject to blocking. The plateau length is limited by after-pulsing in the photomultiplier, an effect that is aggravated by high counting rates.

Tubes $V_7$ through $V_9$ and the associated circuits constitute a trigger circuit whose dead time can be accurately set for 5, 10, 25, 50, and 100 $\mu$sec. The circuit is not new,[3] except for the addition of a panel meter that indicates the percentage of true counting rate on a linear scale calibrated from 0 to 100%. This circuit serves two useful purposes: first, it gives an immediate indication of the dead-time correction to be applied to a measurement; second, it reduces the normal plateau slope when used with some proportional counters by failing to count those spurious pulses which may arise from photon interactions at the counter wall.

Because of its short rise time, good overload properties, and low noise, the amplifier should be particularly well suited for coincidence measurements.

The information presented in this report is the outcome of a request for a counter amplifier by T. A. Gens of the Chemistry Division.

[3]E. H. Cooke-Yarborough, *J. Sci. Instr.* 26, 96 (1949).

## A GATED PULSE-TRAIN GENERATOR

E. Fairstein

One method of quantizing a series of random-height pulses is to cause each of the incoming pulses to trigger a secondary pulse train in which the number per train is proportional to the amplitude of the triggering signal. In this manner, a continuous pulse-height spectrum can be converted to one having a number of discrete levels – a desirable arrangement from the standpoint of information storage.

If the number of pulses per burst is to be linearly related to the amplitude of the triggering pulse, it is necessary that the pulses in the burst be of uniform height and spacing.

A commonly used method of producing a pulse train is to start and stop a sine-wave oscillator by a properly shaped gating signal. The objection to this method is that it is difficult to start a sine-wave oscillator without introducing a transient condition in which the first few oscillations have an amplitude that is different from those occurring after the steady-state condition has been reached. In an alternate method, the oscillator runs continuously, and a gate is interposed between the oscillator and subsequent circuits. The difficulty with this method lies in the fact that there is always an ambiguity of one quantized level associated with the gating operation, since there is no correlation between the time of arrival of the gating signal and the period of the oscillator.

A circuit which has neither of the above shortcomings is shown in Fig. 4. In this circuit, the pulse train is initiated by an incoming signal without the production of a transient amplitude condition, and the pulses are rectangular rather than sinusoidal. Rectangular pulses result in more positive triggering of later circuits than do sine waves.

The circuit operation is as follows: Tube $V_{1b}$ is normally conducting while $V_{1a}$ is cut off. A positive pulse into $V_{1a}$ transfers conduction from $V_{1b}$ to $V_{1a}$ and, in so doing, produces a positive step at the plate of $V_{1b}$. This step is transmitted through the White cathode-follower buffer stage to the input of a delay line that is terminated in its characteristic impedance. The positive voltage step, when it reaches the grid of $V_{1b}$, restores the circuit to its original condition, thus producing a negative step at the plate of $V_{1b}$. This process is repeated for the duration of the gating signal. The repetition period of pulses within a burst is two times the transit time of the delay line. If the amplitude of the voltage step from the delay

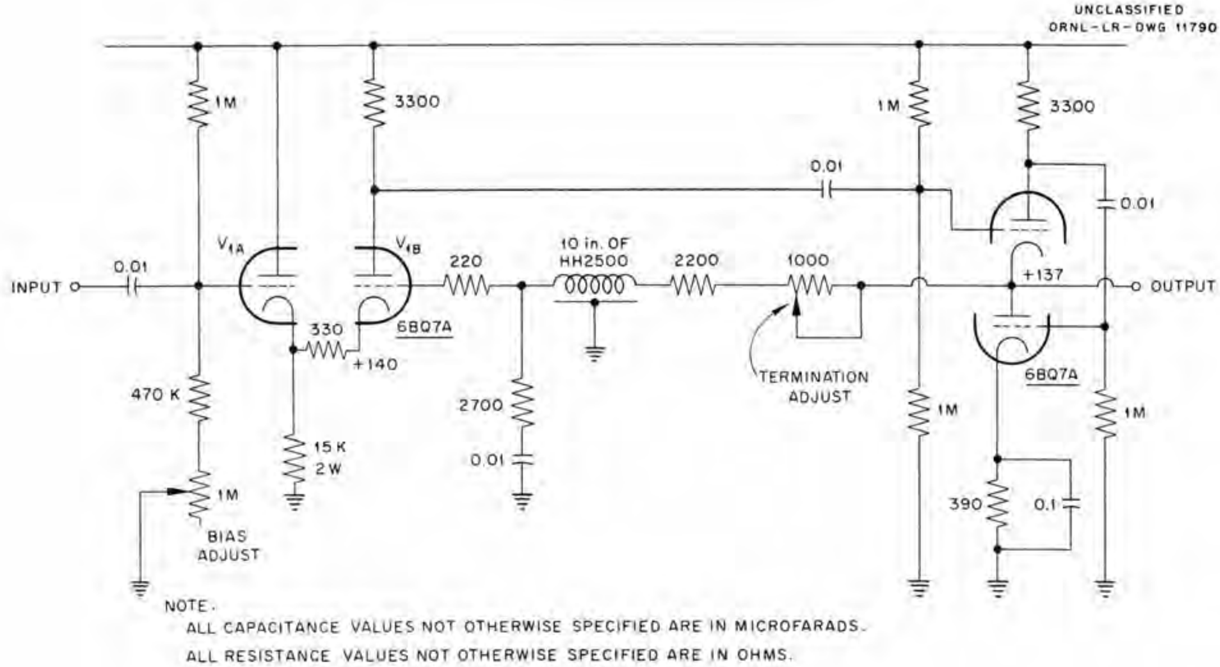


**Fig. 4. Circuit of Gated-Pulse-Train Generator.**

line is sufficient to saturate $V_{1b}$, and if the rise time of the gating signal is less than the rise time of the step from the delay line, the amplitude and period of the first pulse of the train are the same as those of all subsequent pulses.

The circuit of Fig. 4 differs from that of a conventional oscillator in that the feedback around $V_{1b}$ is negative rather than positive. The circuit must not oscillate in an uncontrolled fashion at a frequency where the feedback may become positive due to undesired phase shift in the delay line; therefore, it is necessary to keep the loop gain of $V_{1b}$ at a low level. This is accomplished by the use of an unbypassed cathode resistor.

The circuit will operate with input signal amplitudes of 15 to 50 v. There exists an optimum bias adjustment for a particular gating-signal level, but the adjustment is sufficiently noncritical to allow a fixed resistor to replace the control once the proper setting has been determined.

Figure 5A is an oscillogram of the output signal. This is a multiple exposure; the duration of the gating signal was changed in steps in the range from 2 to 3 $\mu$sec between exposures. Differences between successive pulses are due to the oscilloscope and not to malfunction of the circuit.

Figure 5B is a similar oscillogram showing the output when a much longer gating signal is used.

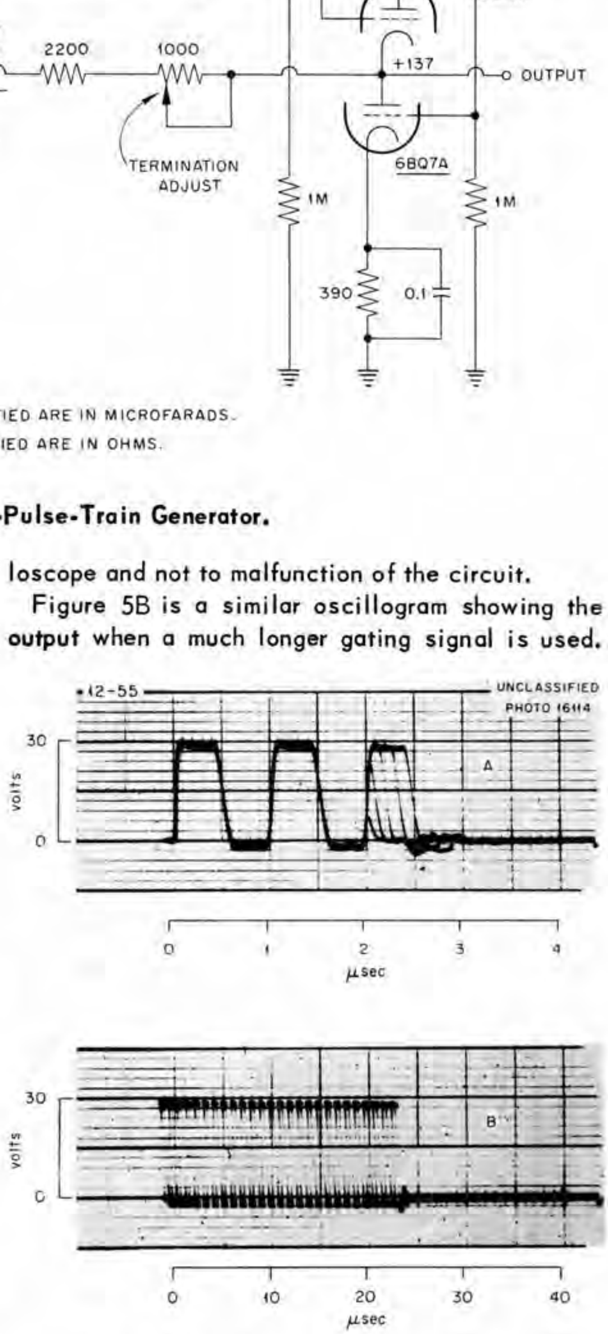


**Fig. 5. Oscillograms of Output Signals.**
(A) Gating signal in 2- to 3-$\mu$sec range;
(B) much longer gating signal.

## THE REACTOR-CONTROLS ANALOG FACILITY

R. S. Stone F. P. Green

The program for enlarging the reactor-controls simulator is now completed. This program included the renovation and consolidation of elements of the original facility, as well as the installation of a linear analyzer and control console from Electronic Associates, Inc. and a double rack of nonlinear components from Reeves Instrument Corp. The installation was engineered by R. A. Dandl, with the major fabrication being done by H. Frazier and other technicians under the direction of H. A. Todd. A large portion of the installation is credited to R. L. Livesey and F. S. Burns of the Reactor Controls Department.

Figure 6 is a photograph of the completed facility. Double-rack A is the Electronic Associates console, which includes the patch bay, control panel, and 20 d-c operational amplifiers, the latter available either as summers or as integrators. All critical passive elements are temperature-controlled in an oven and are held to 0.01% of nominal value. This console also contains two triple-pot servo multipliers.

Double-rack B is the Reeves Instrument nonlinear unit, which contains five electronic multipliers in the left-hand rack and four diode function generators in the right-hand unit. The rack space below the shelf holds the 28 d-c operational amplifiers which are necessary for the functioning of this equipment.

Triple-rack C houses the output equipment and includes four Brown strip-chart and four G-E photoelectric recorders. Rack D holds power supplies for the ORNL-constructed equipment. Rack E contains the 20 operational amplifiers of the original simulator. These are available at the Electronic Associates console patch bay as 20 additional summers. Rack F contains a varied assortment of special-purpose components assembled at ORNL. The small panel at the top of the rack houses a calibration circuit for monitoring the output of the four synchronous delay networks. The large chassis second from the top is a group of precision resistors and condensers available for preparing special transfer functions. The two large dials on the third chassis control two capacitor-storage delay lines for the simulation of multisecond transport lags.

The connector panel tying ORNL components into the patch bay of the Electronic Associates console is located below the time lags. The next

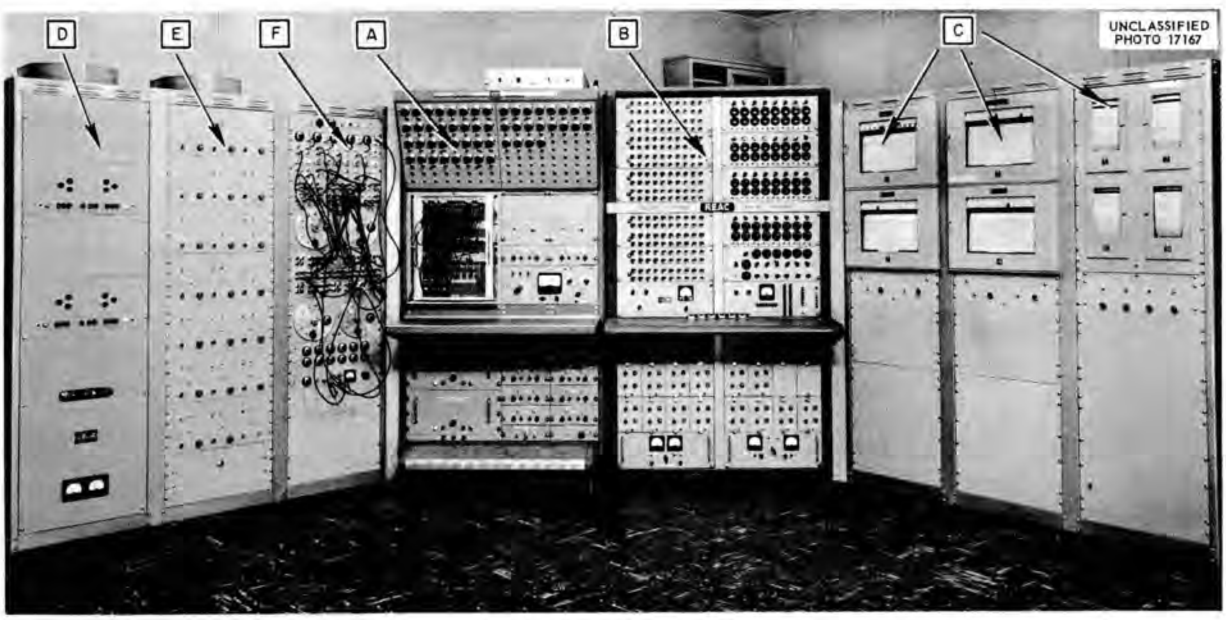


**Fig. 6. Reactor-Controls Analog Facility.**

chassis contains two more synchronous lag lines, and the bottom unit in the rack houses a group of special-purpose feedback circuits, used to simulate the delayed neutron contributions in nuclear reactor problems. This circuit was originally designed by J. J. Stone.[1]

Although the principal function of this equipment is reactor simulation, it can be used for the investigation of a great variety of dynamic situations, embracing, in general, those systems whose behavior is described by a set of linear or nonlinear differential equations in one independent variable. The highest order possible in these equations depends upon the number of terms involved. As indicated previously, a total of 20 operational integrations is possible, although the 20 ORNL summers can also be converted to integrators if the necessity arises.

In this equipment the high-gain d-c amplifier is the basic computing element. By the proper choice of input and feedback impedances, it is possible to make such amplifiers assume the characteristics of a wide variety of transfer functions.

The principal uses of the analog installation include real-time simulation for reactor-component and reactor-control-system design, simulation of typical and new reactor designs for training of ORSORT students and for reactor operations, and accelerated- or retarded-time base computation of dynamics problems in science and engineering. The large number of problems now being handled attests to the versatility of the new facility. Several removable patch boards are available which permit temporary storage of long-range problems while other problems are being solved on the machine. This feature has permitted personnel in other laboratory divisions to investigate systems which are impractical to solve by other means.

Figure 7 illustrates the theory behind the use of amplifiers in electronic analog computers. The amplifiers used are designed around an odd number of stages, so that the output voltage, $-e_o$, is of opposite polarity to the input voltage, $e_o/A$. The gain, $A$, is so high (up to $3 \times 10^8$, depending upon frequency) that it is possible to consider $e_o/A = 0$, with negligible error.

Grid current into the first stage is very low, of the order of $10^{-10}$ amp, and this also is neglected

UNCLASSIFIED
ORNL-LR-DWG 12767

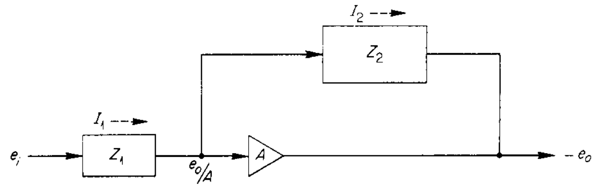


**Fig. 7. Block Diagram of Transform-Function Amplifier.**

in the analysis. Using these approximations,

$$I_1 = \frac{e_i}{Z_1} = I_2 = \frac{e_o}{Z_2} ,$$

or

$$e_o = -e_i \frac{Z_2}{Z_1} .$$

In the case of multiple inputs through a number of input impedances, the output is found to be the sum:

$$e_o = -Z_2 \sum_{j=1}^{n} \left(\frac{e_{ij}}{Z_{1j}}\right) .$$

If $Z_1$ and $Z_2$ represent resistors, the amplifier operates as a constant multiplier, $R_2/R_1$. If $Z_1$ represents a resistor and $Z_2$ a capacitor, the amplifier becomes an integrator, with a time constant of $R_1C_2$. A differentiating circuit is produced by making $Z_1$ a capacitor and $Z_2$ a resistor.

The requirements of most linear systems are satisfied by a combination of summers and integrators, and these are the two types of amplifier operations most readily provided for in the patch bay.

The function generators in the nonlinear system provide for more complex transforms than are readily set up on the patch board. These generators utilize variable bias on a set of diodes to approximate any continuous function by a series of line segments, whose break points and slopes may be varied at will. Figures 8 and 9 illustrate this technique in a typical case. As the magnitude of $x$ increases, the series of diodes reaches a state of conduction, one by one, and changes

[1] J. J. Stone and E. R. Mann, *ORNL Reactor Controls Computer*, ORNL-1632(Rev.) (March 1, 1956).

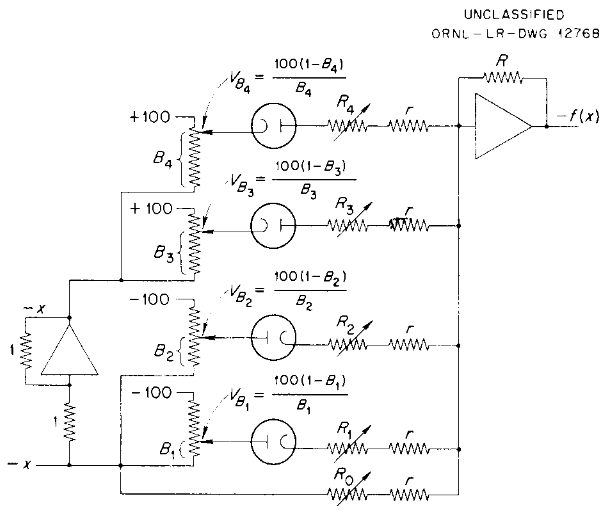


**Fig. 8. Schematic Diagram of Function Generator.**

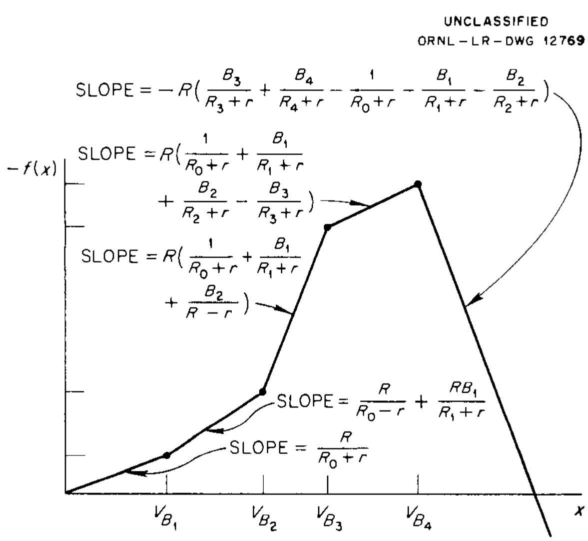


**Fig. 9. Input/Output of Function Generator.**

the summing junction potential of the output amplifiers. Selector switches on the unit permit necessary reversal of the polarities of the input voltages and the orientation of the diodes. This is illustrated in Fig. 8, where the first three segments increase the slope of the function, and the last two segments diminish the slope. Break points, $V_B$, are controlled by the $B$ potentiometers, which vary the amplifier gain for each segment.

Figure 9 shows the type of transfer function to be expected of the generator connections in Fig. 8.

The electronic multipliers complete the nonlinear unit, and, as their name implies, each of these units provides a product of two variables. The Reeves multiplier works on the quarter-square principle and is built around two diode-function generators of the type just described.

Figure 10 shows the block diagram of these multipliers. From Fig. 10 the following relations can be obtained:

1. Amplifier No. 1 adds $\frac{y}{2}$ and $\frac{x}{2}$ to give $-\left(\frac{x+y}{2}\right)$.

2. Amplifier No. 2 adds $-\left(\frac{x+y}{2}\right)$ and $x$ to give $\frac{y-x}{2}$.

3. Function generator A operates on $-\left(\frac{x+y}{2}\right)$ to give $-(x+y)+\frac{(x+y)^2}{400}$.

4. Function generator B operates on $\frac{y-x}{2}$ to give $(y-x)-\frac{(y-x)^2}{400}$.

5. The outputs from the two function generators are added to $2x$ in amplifier No. 3 to give $(x+y) - \left(\frac{x^2+2xy+y^2}{400}\right) + (x-y) + \left(\frac{x^2-2xy+y^2}{400}\right) - 2x$ or $-\frac{xy}{100}$.

Identical results could be more easily obtained by generating and then adding together the functions $-\left(\frac{x+y}{2}\right)^2$ and $\left(\frac{y-x}{2}\right)^2$ to achieve $-\frac{xy}{100}$ at the output. However, in this case the points of inflection of the parabolas approximated in the function generators would lie at the origin, where a given error in voltage is percentagewise at its greatest. The junctions actually chosen by the manufacturer place the point $x = 0$, $f(z) = 0$, in a region of slow monotonic increase in slope.

Division of the product by 100 ensures that the product can never exceed the 100-v operating range even if both $x$ and $y$ approach a value as high as 100 v.

The expanded analog facility has been placed in operation and has proved successful in the investigation of problems involving reactors and other systems of interest to the Laboratory.

UNCLASSIFIED
ORNL-LR-DWG 12770

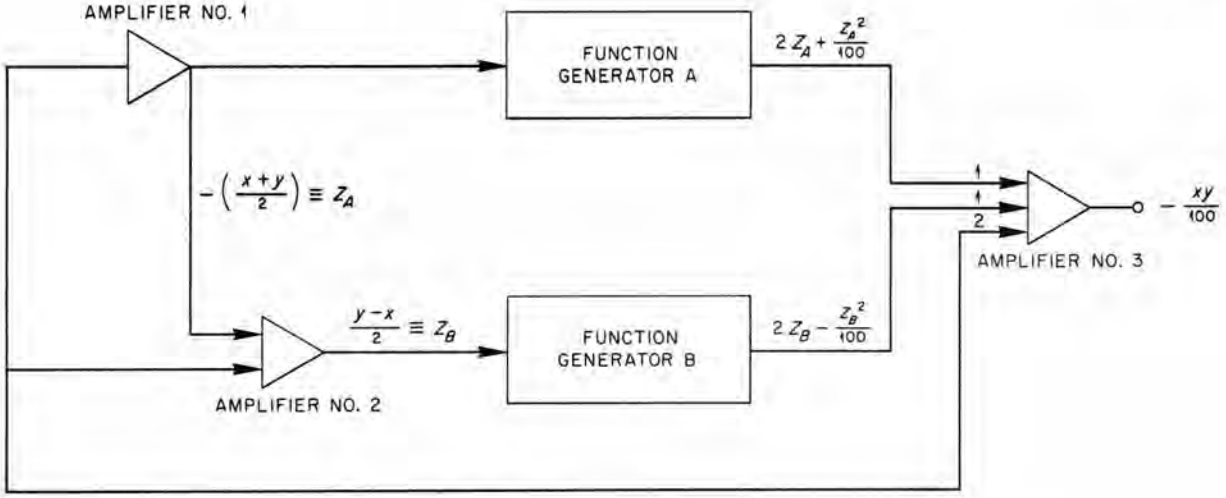


**Fig. 10. Block Diagram of Electronic Multiplier.**

---

## CATHODE-RAY-TUBE OUTPUT DEVICE FOR THE ORACLE

R. J. Klein

The cathode-ray-tube output unit for the Oracle has been completed and placed in service. Facilities are provided for temporary visual and permanent photographic information output in the form of graphs (see Fig. 11) or lettered sheets which are similar to printed pages. Both outputs are extremely fast compared with more conventional punching and printing devices. For example, in order to plot a point on a graph, it was formerly necessary to punch two numbers for the coordinates of the point, which required about 1 sec of machine time, then locate this point on graph paper and make a pencil dot. Now, the entire operation is accomplished by the machine in about 200 $\mu$sec. It is possible to plot a complete graph with axes and labeling in less than 1 sec. The curve-plotter camera has a film capacity of 200 exposures.

Special circuitry has been incorporated which provides semiautomatic letter plotting at a maxi-

UNCLASSIFIED
ORNL-LR-DWG. 12771

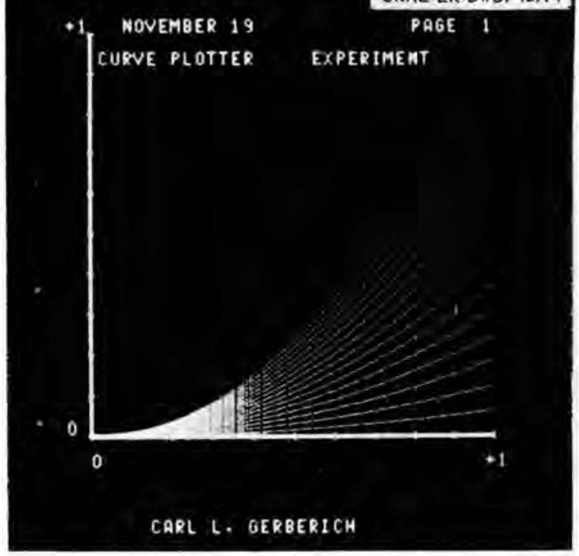


**Fig. 11. Display Sample for Cathode-Ray-Tube Output.**

mum speed of 2000 letters/sec. This circuitry also makes coding for letter plotting easier than that required for the point-by-point methods.

The linearity of the resulting graphs is within 1%, and most of this error is caused by the nonlinearities of the plotting tube itself.

---

## AUTOMATIC GAMMA-RAY DECAY RECORDER, MODEL Q-1753

F. M. Glass

The Q-1753 was designed and constructed for F. C. Maienschein and K. M. Henry and is to be used as a means of recording the gamma-ray dose decay over a 16-hr period following a reactor shutdown. A high degree of accuracy is achieved over seven decades by using a linear instrument and automatically changing the integrating time.

The instrument consists of an ion chamber, a Q-1259 d-c integrator, a modified Berkeley model 5510-C universal counter and timer, a Q-1753 timer and gate, and a Berkeley model 1452 digital recorder (see block diagram, Fig. 12).

The operating principle is as follows: The ion current from the chamber is integrated by the d-c integrator, which, in turn, feeds one pulse for every 0.1 $\mu$coulomb into the 5510-C counter and timer. One-second timing pulses from the 5510-C are fed through the 1-sec gate in the Q-1753 timer and back to the 5510-C, allowing the 5510-C to count for 1-sec intervals. At the conclusion of a 1-sec counting interval the next pulse stops the counting process and starts the printing cycle of the digital recorder. The next timing pulse resets the decade counting units and initiates another counting cycle. Thus, during the first 10-sec interval, five counts are made and recorded at 2-sec intervals. At the end of the first 10-sec interval, the 1-sec gate closes and the 10-sec gate opens, allowing only timing pulses that have been scaled down by a factor of 10 to pass through the 10-sec gate. Thus the counter counts 10-sec intervals. This process is repeated for the 100- and 1000-sec intervals for the remainder of the run.

UNCLASSIFIED
ORNL-LR-DWG 12772

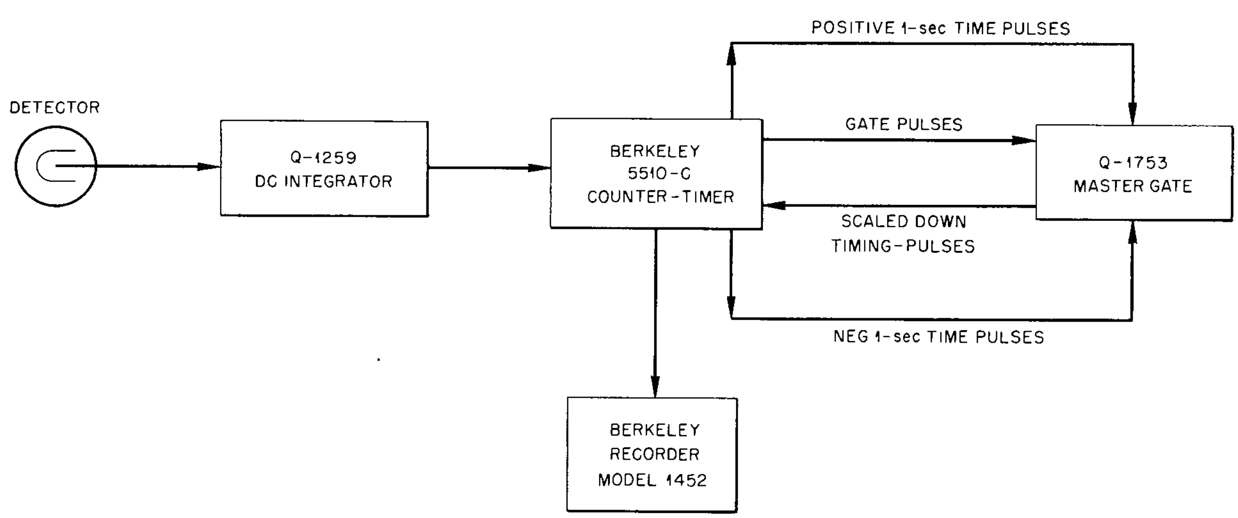


**Fig. 12. Block Diagram of Q-1753 Automatic Gamma-Ray Decay Recorder.**

Although the range of the Q-1259 integrator is adequate for the seven decades, the timing scheme described is used in order to provide sufficient counting time for good statistics at the lower end of the decay curve without exceeding the storage capacity of the Berkeley counter at the high end of the curve.

The automatic timing is synchronized with the reactor scram by using the input gate signal in the counter to trigger the scram signal generator. This gate signal simultaneously resets all the timing units.

Manually operated gate switches allow the operator to disable the timing sequence, making possible continuous operation on any of the available time bases while the reactor is in operation.

---

## ULTRASONIC POWER AMPLIFIER AND PICKUP, MODEL Q-1741

F. M. Glass

The Q-1741 was designed and constructed for M. T. Morgan and is to be used in mechanical vibration studies. The instrument consists of a sine-wave generator, a power amplifier, an electrostatic transducer used as a driver, an electrostatic pickup, and a preamplifier and amplifier with built-in level meter (see block diagram, Fig. 13).

The frequency response of all three amplifiers is flat to ±1 db from 10 to 200 kc. The power amplifier delivers to the electrostatic driver a sine wave whose amplitude may be as great as 1300 v peak-to-peak. The sample serves as a plate that is common to both the driver and the pickup, and both components are housed in a vacuum chamber. This system has been used successfully to observe and record harmonic peaks whose frequencies may be as high as 750 kc.

UNCLASSIFIED
ORNL-LR-DWG 12773

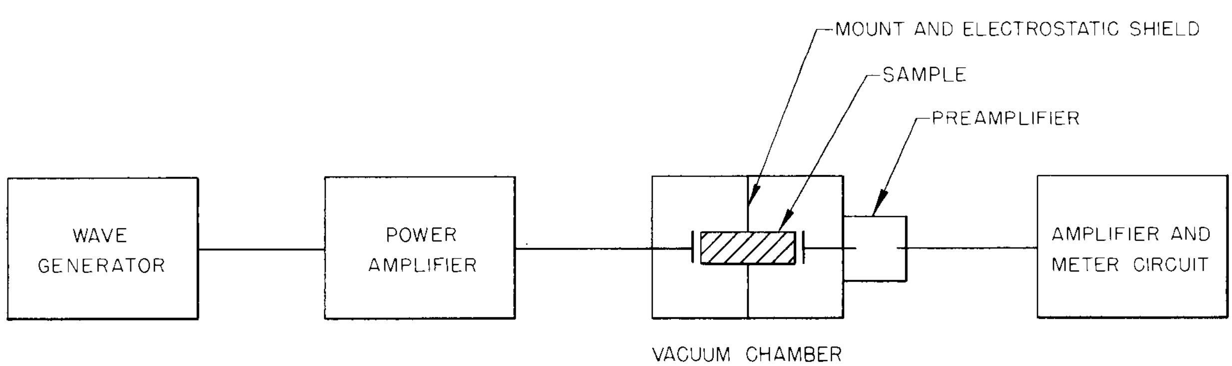


**Fig. 13. Block Diagram of Q-1741 Ultrasonic Power Amplifier and Pickup.**

## VIBRATION ANALYZER, MODEL Q-1744

F. M. Glass

The vibration analyzer, Q-1744, was designed and constructed for D. O. Thompson and is to be used in the study of the moduli of elasticity of various metals. The instrument simplifies the measurement of the radiation effects on the internal damping of metals that are being irradiated in the ORNL Graphite Reactor. The complete system consists of the components shown in the block diagram, Fig. 14.

### Operation

In this system, the transducer, sample, transmitter, receiver, compressor amplifier, and power amplifier comprise a closed loop. When properly phased, this loop starts and sustains oscillation at the natural vibrating frequency of the sample. The automatic gain-control amplifier compares the output of the f-m receiver with a d-c reference voltage and supplies a bias voltage proportional to the error voltage to the compressor amplifier. The gain of the compressor amplifier is therefore automatically controlled to maintain a driving power to the transducer that will produce a constant output at the receiver. Any change in the moduli of elasticity is indicated as a driver current change and is recorded on a strip-chart recorder. The resonant frequency of the sample is measured by comparing the signal in the loop with a reference signal. The beat frequency is counted by a linear-count-rate meter and recorded on a second strip-chart recorder. This makes possible a long-period chart recording of resonant frequency changes of the sample as a function of its environment. The two signals can be viewed on a built-in 2-in. oscilloscope and appear as a liaison figure.

The sample under test serves as one plate of the tank condenser in the transmitter and thus provides direct frequency modulation. The receiver has sufficient automatic frequency control to compensate for slight frequency shifts caused by temperature deviations and for minor mechanical instabilities in the transmitter.

UNCLASSIFIED
ORNL-LR-DWG 12774

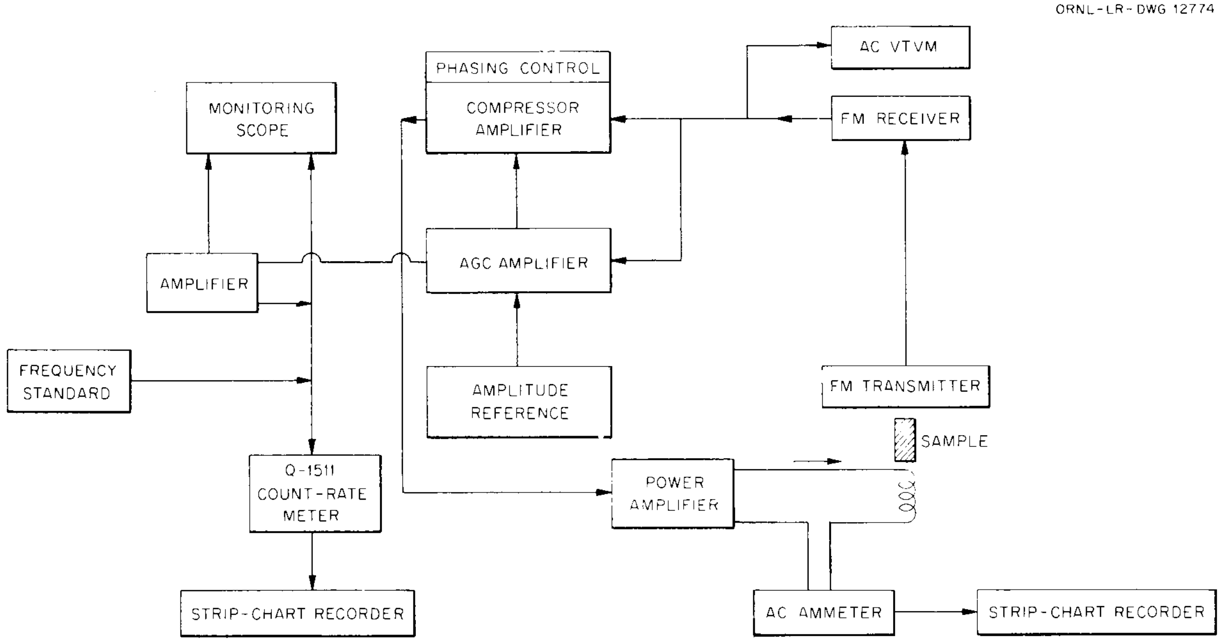


Fig. 14. Block Diagram of Vibration Analyzer, Model Q-1744.

## ENERGY RESOLUTION OF THE ORNL 3-Mv VAN DE GRAAFF

J. P. Judish C. H. Johnson R. F. King

The energy resolution of the ORNL 3-Mv Van de Graaff was measured by observing the thick target yield of the 993.3-kev $Al^{27}(p,\gamma)$ resonance, which has a natural width of the order of 100 v.[1] The beam was analyzed by a 90-deg bending magnet whose field was continuously monitored with a nuclear magnetic-resonance device. The magnetic field could be set and held at a given value within 0.003%. Variations in beam energy caused by changes in the magnet analyzer field were therefore less than 0.006%. Van de Graaff voltage control is achieved by feeding back, through an amplifier to the grid of a triode tube, the signal from a pair of slits located 40 cm from the magnet output face. The triode plate is connected in series with a set of corona points which supply current to the Van de Graaff terminal. A 17-$\mu$a beam emerging from the magnet was allowed to impinge on a target cooled by liquid nitrogen. The gamma-ray yield was monitored with a NaI(Tl) crystal mounted on a photomultiplier tube. A determination was made of the full width at half-maximum of the gamma-ray peak as a function of control slit spacing and corona amplifier sensitivity. For the best energy resolution it was found that this sensitivity should be set just below the point where the corona triode begins to overdrive. A small increase or decrease in amplifier sensitivity would increase the gamma-ray peak width as much as $1\frac{1}{2}$ times. The slit spacing for the best energy resolution was found to be 50 mils. When the slit spacing and amplifier sensitivity were set at optimum, the full width at half-maximum of the gamma-ray peak was 200 ev. This is about 16 times better than that expected from an analyzing magnet which has the same geometry as the one used in this experiment but which analyzes a beam with a continuous energy spread. Visual observation of the beam on a quartz viewer just preceding the target disclosed a periodic beam-position jitter. This indicates that the terminal voltage changes with a definite period and may possibly be associated with belt modulation. This periodic voltage change may account for much of the beam energy spread.

[1] R. S. Bender *et al.*, *Phys. Rev.* **76**, 273 (1949).

## A PULSED ION SOURCE FOR THE ORNL 3-Mv VAN DE GRAAFF

R. F. King J. P. Judish H. E. Banta

The ion-beam pulser described by Parker and King[1] has been installed in the terminal of the ORNL 3-Mv Van de Graaff. Since the elements of the pulser consist of two sets of beam-deflector plates and an Einzel lens, the pulser in no way interferes with normal operation of the Van de Graaff machine. When unpulsed beams are required it is necessary to turn off the radio-frequency oscillator supplying the deflecting voltage. With the application of sine-wave r-f voltage of the proper frequency and amplitude, ion-beam bursts less than $10^{-8}$ sec in duration have been produced. Pulse repetition rates of 1 $\mu$sec have been used which correspond to an oscillator frequency of 0.5 Mc/sec. The resulting over-all resolution of the machine is $6.6 \times 10^{-9}$ sec, as measured by means of the $Li^7(p,p'\gamma)$ reaction (see Fig. 15).

[1]V. E. Parker and R. F. King, Abstract No. Y-8, *Am. Phys. Soc. Bull.* 1, Series 2, 70 (1956).

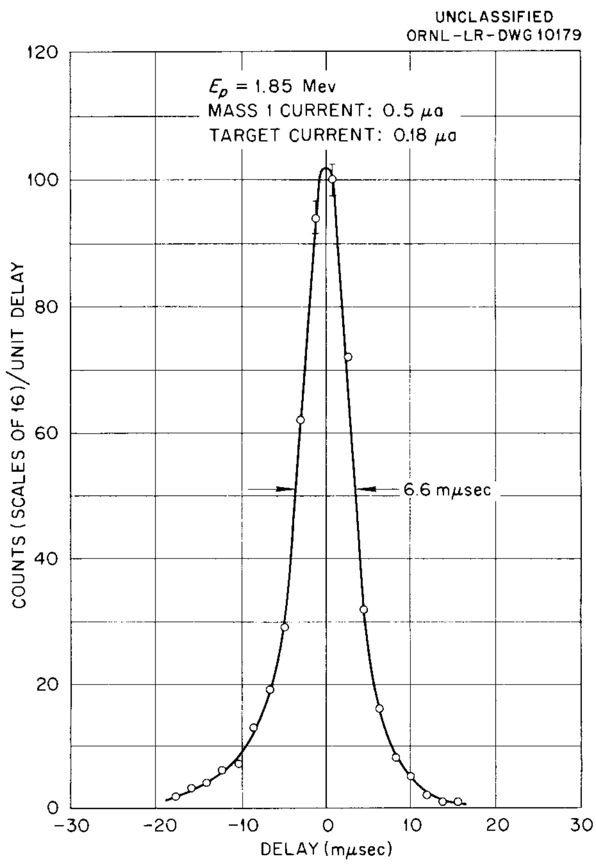


**Fig. 15. Ion Beam Pulser Over-all Resolution Test on $Li^7(p,p'\gamma)$.**

---

## INSTRUMENTATION FOR THE 8-in. MASS SPECTROGRAPH

R. D. Sidnam

Instrumentation for the 8-in. mass spectrograph utilizes a counting system which uses two readouts. One readout consists of a linear-count-rate meter and a Brown strip-chart recorder for peak plots, and the other consists of a counter-timer-printer for tape tabulation. The approximate current range of the counting equipment is from $10^{-14}$ to $10^{-20}$ amp. An electron multiplier is used to amplify charged ions from the beam current to an amplitude sufficiently high to drive an amplifier. The amplified output is then fed to the linear-count-rate meter (Q-1511) and displayed on the recorder (see block diagram, Fig. 16).

The magnetic-field sweep rate is closely linked to the equilibrium time of the count-rate meter which actually fixes the response time of the

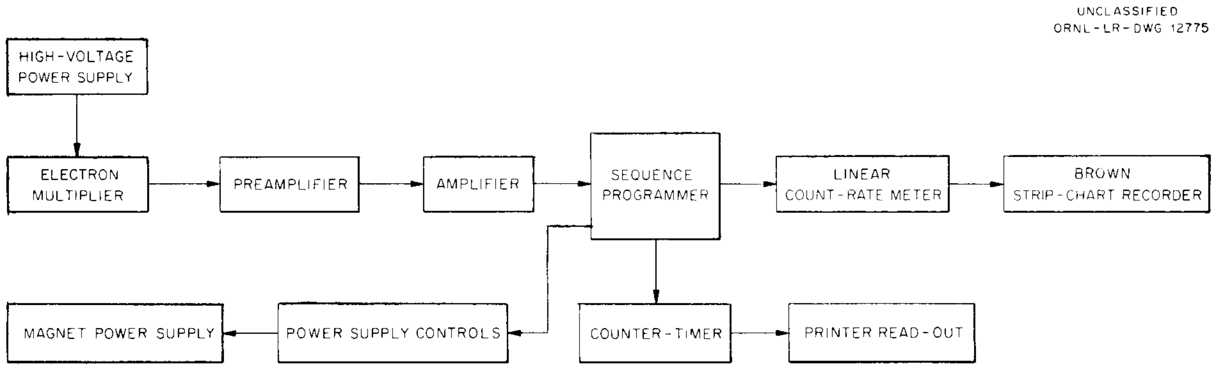


**Fig. 16. Block Diagram of 8-in. Mass Spectrograph Instrumentation.**

system. In general, for a fixed count rate, a shorter response time of the count-rate meter allows a faster field sweep, but the standard deviation of the count rate is greater.

As shown in Fig. 16, the strip-chart plot of the peaks results from the interactions of the detector, amplifier, sequence programmer, linear-count-rate meter, recorder, and magnet-power-supply controls. Scanning can be either manual or automatic. In the automatic setting, the field is scanned in one direction until a value set by one control Helipot is reached, then the direction is reversed and the field is scanned in the opposite direction at the same rate until a value is reached that has been set on the other control Helipot. A push button is provided for a fast sweep that facilitates setting the upper and lower limits. Manual scanning can be accomplished by either of the two Helipots ($M_1$ and $M_2$). Since the recorder chart speed is constant, a wide selection of magnetic-field sweep speeds can be obtained to give good peak shapes. A large number of recorder ranges can be obtained by combining the range selector on the linear-count-rate meter and the scaling factors that are available on the sequence programmer.

In the second data-collecting system, a counter-timer and printer is operated in the following manner:

1. As an abundance-ratio recorder, the $M_1$ and $M_2$ controls are manually set to the two mass numbers of interest. The sequence controller is then set to the "step" position, which causes the magnet field to switch alternately between the two mass numbers. Counts can be accumulated either on a preset-time basis or a preset-count basis. If the switching time is made small compared with the drifts in the system, the error introduced by the drifts on the determination of the abundance ratio is minimized.

2. The scaler-printer system can accumulate data to a given statistical accuracy in approximately half the time possible with a rate meter and recorder system and is therefore well suited to low-beam-current operation.

The maximum timing interval that can be used with this equipment is 10 sec. The number of counts registered during this interval is printed on the tape. Both preset count and preset time require that the tape be summed for an equal number of steps for each peak.

## A THYRATRON POWER SUPPLY FOR ELECTROMAGNETIC STIRRING

B. C. Behr

A special d-c power supply for stirring liquids electromagnetically has been developed for A. R. Jones and W. M. Woods of the Chemical Technology Division. This device switches up to 15 amp, at 0 to 120 v, alternately to two output terminals at rates from 0.5 to 20 cps.

An iron-core stirring plunger located inside a stainless steel vat that contains the liquid is magnetically coupled to two externally wound solenoid coils, which, if alternately energized, transduce an oscillatory linear motion to the iron core.

Because of the inefficient magnetic coupling from the solenoids to the stirring plunger, large currents are required in the coils to achieve stirring action. The switching mechanism is therefore subjected to severe strain. Previously used mechanical switching devices, such as cam-driven switches and relays, have proved to be unsatisfactory after a few days of operation because of electrical or mechanical failures.

The thyratron power supply is shown in a block diagram (Fig. 17). The device consists of a variable-frequency linear saw-tooth generator, an amplitude discriminator, a flip-flop circuit, two free-running blocking oscillators, and the power thyratrons which receive their plate voltage from a variable transformer. The basic switching frequency, set by the saw-tooth generator, is adjustable from 0.5 to 20 cps and is constantly monitored by the frequency meters. Division of power between the two output terminals is controlled by the amplitude discriminator. A biasing arrangement on the input grid of the d-c coupled flip-flop raises or lowers the triggering level of the saw-tooth waveform, thereby setting the duration of each half cycle of the flip-flop. Depending upon which plate of the flip-flop is off, one or the other of the blocking oscillators becomes regenerative. This action pulses the grid of the oscillator's corresponding power thyratron with a series of high-frequency, large-amplitude pulses, causing it to conduct. Within a given switching cycle, a load-division control allows continuous on-off variation from 10 to 90% at either terminal with a linearity of 1 to 8%, depending upon the frequency. Load current is adjusted by limiting the applied 60-cps plate voltage of the thyratron.

Performance of the power supply during the first two months of operation has been satisfactory. Also, because of the versatility of control, it was found possible to make relative viscosity measurements of the stirred liquid.

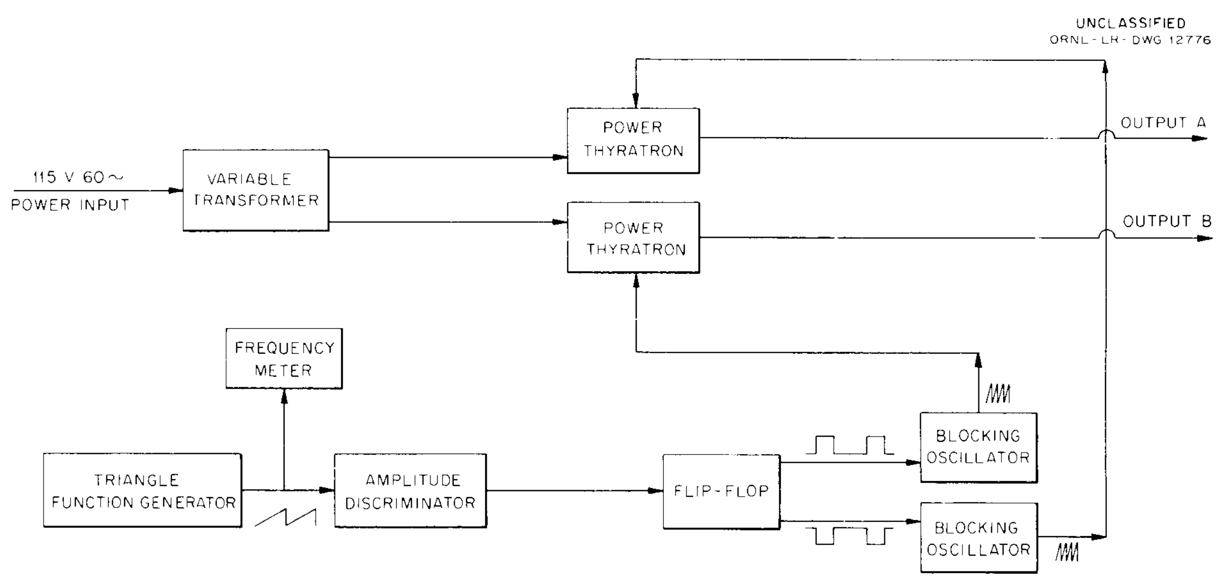


**Fig. 17. Block Diagram of Thyratron Power Supply.**

## A SUBMINIATURE TUBE DRIVER FOR GLOW-TRANSFER TUBES

F. M. Porter H. J. Hurst

The circuit shown in Fig. 18 was developed to drive the GC10B glow-transfer tubes used in the 60-channel pulse-amplitude analyzer. In this application, simplicity, lower power consumption, and reliability were of primary importance, since there would be several hundred such units constructed.

The transfer of the glow from one stable position to the next is accomplished by applying, successively, large negative pulses to the guide electrodes which are labeled 1 and 2 in the circuit drawing. In response to an input trigger pulse the 1AG4 plate potential drops rapidly. The potential of guide 1 follows this drop until it is about 40 v negative with respect to the initial stable position, at which point the glow shifts from the stable position to guide 1 and begins charging the series capacitor. During the charging time interval the potential of guide 2 drops at a rate determined by the associated RC time constant. As guide 2 becomes negative with respect to 1 the glow shifts from 1 to 2. With the glow transferred to guide 2 there exists an approximate balance between the currents in 1 and 2 such that the potentials of these electrodes do not change appreciably until the 1AG4 input signal disappears. When the plate current of the 1AG4 tube is cut off, the balance at guide 2 no longer exists, and its potential increases positively. It should be noted that guide 1 is maintained less negative than 2 while the glow is on guide 2. Furthermore, as the potential of 2 increases, the potential of 1 will increase an equal amount without a time delay.

When the potential of guide 2 has increased to a value that is positive with respect to the following stable position, the glow will shift to this position.

This completes the transfer of the glow from its initial stable position to the following stable position in response to a single trigger pulse. Since the input trigger pulse is sufficiently large to drive the 1AG4 tube to saturation and since the glow transfer from guide 2 to the following stable position takes place at a definite potential, the entire drive circuit has d-c restoration after each trigger pulse.

The carry pulse obtained upon the glow transfer from the nine-to-zero position is about 27 v and does not change in shape, irrespective of the number of decades connected in series. Figure 19

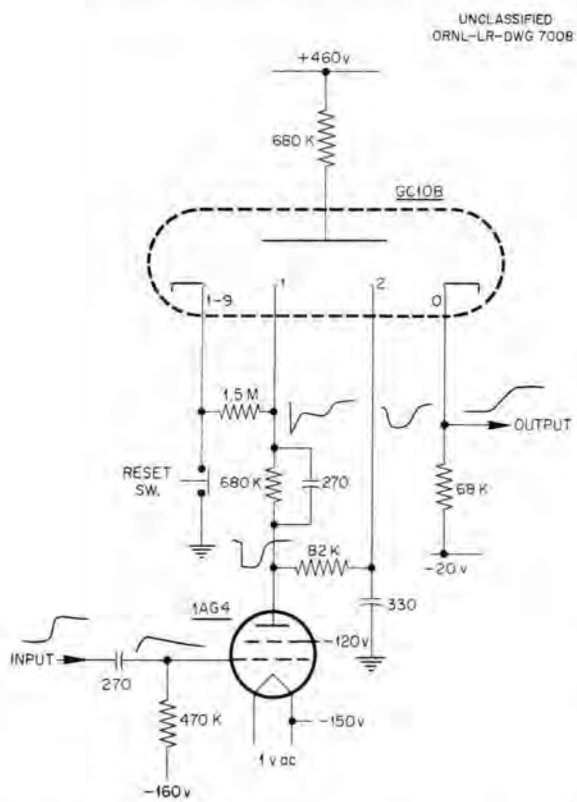


**Fig. 18. Circuit of Glow-Transfer Decade Scaler.**

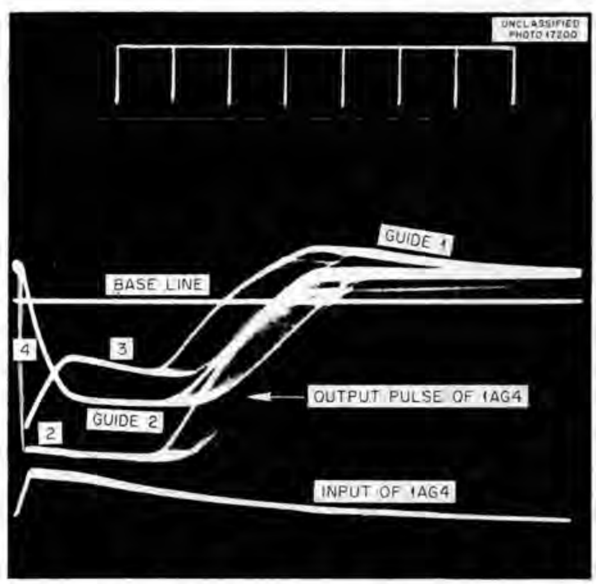


**Fig. 19. Oscillograph of Pulses at Various Points in Circuit.**

is a photograph of the pulses at various points in the circuit.

This circuit has proved to be very adaptable to multichannel construction, consumes less than 0.2 w per decade, and is insensitive to very large excursions of the supply voltages. In January 1955, there were 240 such units constructed and placed in operation. To date there have been only two GC10B failures and no 1AG4 failures.

---

## A 60-CHANNEL PULSE-AMPLITUDE ANALYZER

F. M. Porter H. J. Hurst
C. J. Borkowski J. R. Tarrant

A 60-channel pulse-amplitude analyzer using an electron beam tube as the pulse-amplitude encoding device[1] was constructed and has been in operation since January 1955. It should be recalled that the electron-beam tube consists of a conventional electron gun in front of which has been placed a target grid having equal open and closed spaces. Directly behind this grid is placed a collector plate which has a secondary emission ratio of approximately 6 for 2-kv electrons.

The analyzer system (block diagram, Fig. 20) consists of the following elements: a normally closed linear input gate, an internal analyzer bias control, the beam-deflection encoding tube, a two-decade pulse counter with its associated matrix of channel-selecting gate lines, and 60 separate channel-storage scalers (Fig. 21), each consisting of five glow-transfer-type decade counter tubes.

The 60-channel analyzer and associated DD2 linear amplifier shown in Fig. 22 are contained in a single cabinet with provisions for connecting external counters to determine the number of pulses presented to the analyzer during a counting interval. The threshold of the input control circuit is fixed near zero and does not vary with counting rate. The input gate opens to admit a pulse in response to the control circuit. The control circuit may be triggered by the amplifier pulse or an auxiliary coincidence pulse, except during the analysis period, which extends 100 μsec after a pulse is admitted. The internal-analyzer bias voltage corresponds to the lower edge of the first channel and is variable over the range of amplifier pulse amplitudes. Fixed channel widths of 0.25, 0.50, 1.00, and 1.5 v are provided by a gain control on the driver amplifier. The glow-transfer tube dead time does not limit the peak channel counting rate, and the channel storage capacity of $10^5$ counts per channel has proved adequate. An automatic decimal printout for the storage is being constructed which will require about 1 min to print out the 60 channels.

At integral counting rates of approximately 200,000 counts/sec the analyzer accepts about 10,000 counts/sec (which is the rate determined by its fixed analysis time) and sorts these pulses without distortion of the amplitude spectrum. Since there are known distortions of the spectra in the photomultiplier tube, a separate check of the analyzer calibration was obtained by using a coincidence-pulse-generator technique. With this method, the generator pulse is mixed with the random detector pulses at the amplifier input, and the multichannel storage is interrogated only by the generator pulses. As the rate was varied from 100 to 200,000 counts/sec the generator pulse-amplitude shift was about 0.5%, which is the shift observed in using a fast single-channel analyzer.

This analyzer has been in operation approximately 2000 hr since its completion and has proved to be stable and trouble-free, with the following exceptions: It has been necessary to replace three of the GC10D glow-transfer tubes that are used in the input decades of the channel storage, and failure of seven GC10D tubes has been observed when the anode supply voltage is dropped more than 10%. Also, two of the GC10B glow-transfer tubes used in the fourth decade failed by locking in the zero position. (This effect results in a

[1] F. M. Porter, H. J. Hurst, and C. J. Borkowski, ORNL-1674 (March 25, 1954) (Secret).

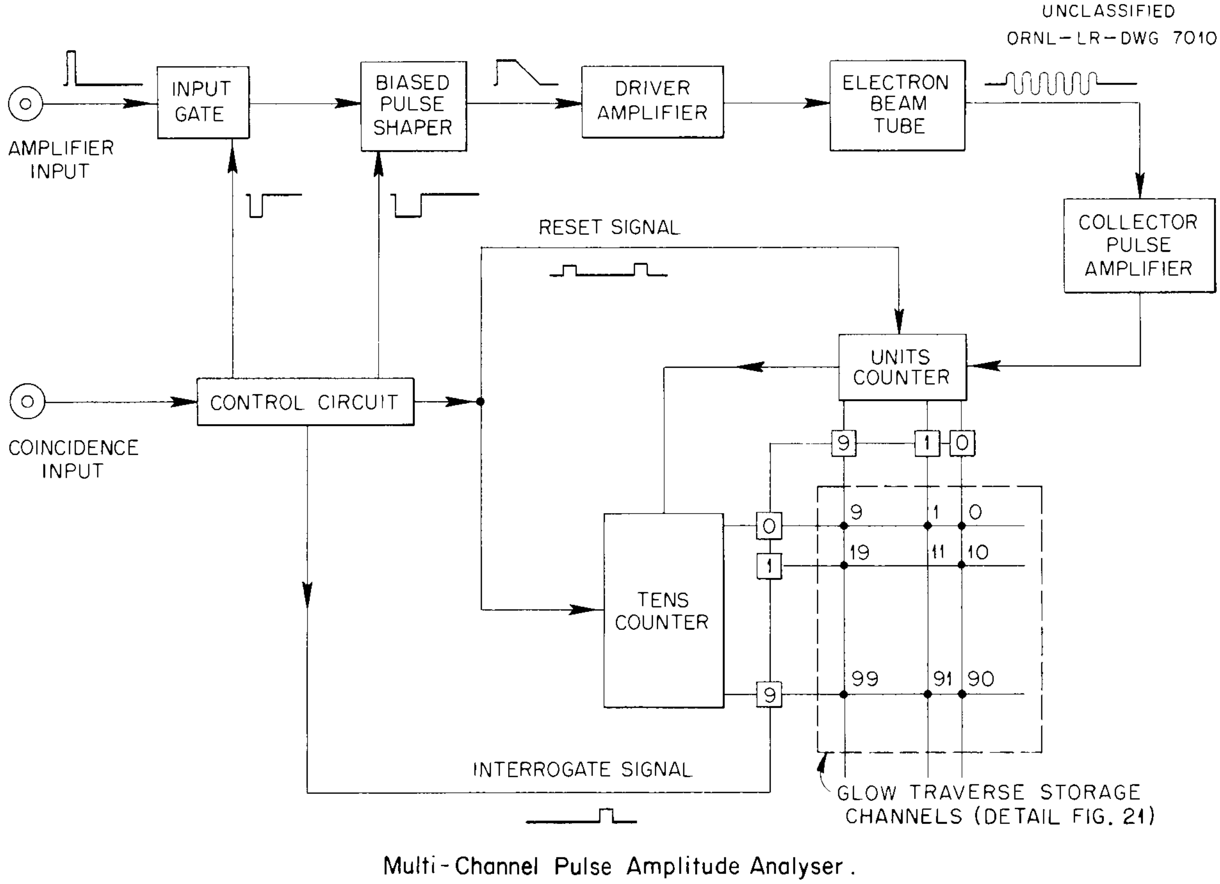


**Fig. 20. Block Diagram of Multichannel Pulse-Amplitude Analyzer.**

scale-through to the fifth decade.) There have been no failures in the 300 1AG4 subminiature vacuum tubes used to drive the glow-transfer tubes. One vacuum-tube failure in the control circuit and one resistor failure were observed. The channel widths have remained constant, and the analyzer zero drift was about 1% per month. The analyzer is turned off each night (unless an overnight run is planned) and turned on again each morning, with no evidence of appreciable drift after a few minutes of operation.

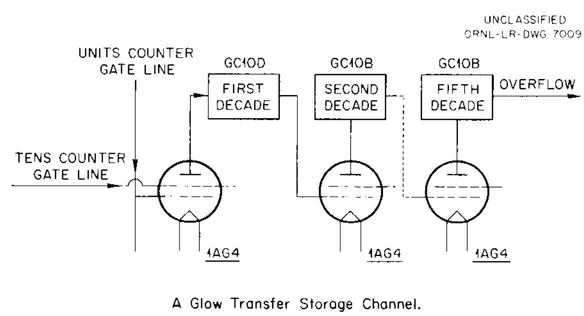


**Fig. 21. Glow-Transfer Storage Channel.**

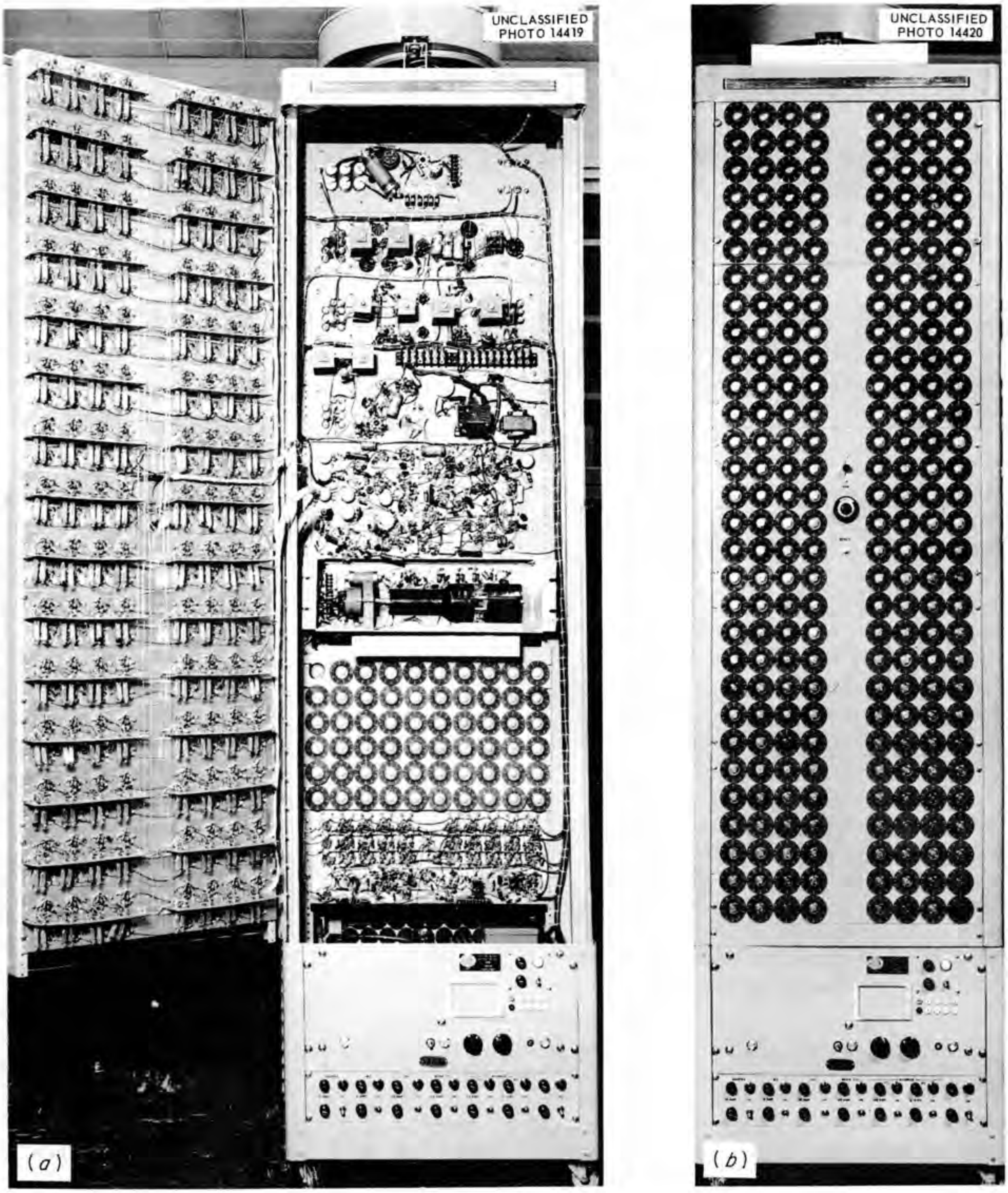


**Fig. 22. The 60-Channel Analyzer.** (*a*) Internal view; (*b*) panel view.